

**The effect of pulsed electrical currents on the formation of  
macrosegregation in solidifying Al - Si hypoeutectic phases**

Zhang, Y.; Rübiger, D.; Willers, B.; Eckert, S.;

Originally published:

June 2016

**International Journal of Cast Metals Research 30(2017)1, 13-19**

DOI: <https://doi.org/10.1080/13640461.2016.1174455>

Perma-Link to Publication Repository of HZDR:

<https://www.hzdr.de/publications/Publ-22859>

Release of the secondary publication  
on the basis of the German Copyright Law § 38 Section 4.

# The effect of pulsed electrical currents on the formation of macrosegregation in solidifying Al - Si hypoeutectic phases

Yunhu Zhang, Dirk Rübiger, Bernd Willers and Sven Eckert\*

*Institute of Fluid Dynamics, Helmholtz-Zentrum Dresden-Rossendorf, 01314 Dresden, Germany*

**Abstract:** Within this study we conducted experimental investigations focusing on the formation of macrosegregation in Al-7wt-%Si alloys exposed to electric current pulses (ECP) during solidification. The distribution of eutectic phase was measured on various sections of the solidified samples. The results do not show the formation of reproducible segregation pattern which can be related to the flow structure generated by ECP. This finding can be ascribed to the turbulent character of the flow, the equiaxed growth of free-moving crystals and a non-symmetric distribution of the electromagnetic force due to an uneven wetting of the electrodes. An increasing input of energy by ECP enhances increases the variations of phase distribution over a longitudinal section.

**Keywords:** Al - Si alloys; solidification; electric current pulse; macrosegregation; melt convection.

## 1. Introduction

Macro segregation in metal alloys is the consequence of solute rejection at the propagating solidification front and its redistribution in the mushy zone during the solidification process <sup>1</sup>. Distinct segregation of solute on macro-scale causes heterogeneous mechanical properties that can dramatically deteriorate the quality of products. Hence, it is of high practical importance and industrial relevance to better understand and to control the formation of macrosegregation.

The distribution of solute is heavily influenced by convective transport in the liquid melt during solidification <sup>2-5</sup>. Many previous investigations have shown that uncontrolled flows arising from natural convection or melt stirring carry the risk of inducing severe macrosegregation effects in solidifying ingots <sup>6-10</sup>. Many studies were conducted so far with respect to electromagnetic stirring by means of a rotating magnetic field (RMF) or a traveling magnetic field (TMF). Zimmermann et al. <sup>6</sup> found that the RMF-induced forced flow generated an axial macro segregation (rich silicon) in the central part of a directionally solidified Al-Si7-Mg0.6 alloy. Zaïdat et al. <sup>7</sup> reported the formation of pronounced segregation freckles during directional solidification of Al-3.5wt-%Ni alloy under the influence of a TMF. Noepfel et al. <sup>8</sup> simulated the macrosegregation formation in directionally solidified alloys under the

---

\* Corresponding author. Tel.: (0351) 260 - 2132, 3563.

E-mail address: s.eckert@hzdr.de.

Post address: POB 51 01 19, 01314 Dresden, Germany

presence of both RMF or TMF and demonstrated a correlation between the macrosegregation pattern and the forced flow structure. A special design of the flow structure in the vicinity of the solidification front by means of tailored magnetic fields has been proposed to control the solute distribution at the solidification front. For instance, a novel approach to suppress macrosegregation in solidifying Al-Si alloy ingots by applying a time-modulated RMF was suggested by Willers et al. <sup>9</sup>. Recently, Jie et al. <sup>10</sup> performed a series of solidification experiments exposed to an RMF and proposed a related segregation mechanism for the formation of Si-enriched layer in Al-Si hypereutectic phase ingot.

During the recent fifteen years the application of electric currents came into the focus as a new tool for manipulating the microstructure and properties of solidified metal alloys. Especially, the grain refining effect of strong electric current pulses (ECP) aroused the interest of many researchers <sup>11-14</sup>. Other studies reported on the improvement of the carbon segregation in steel <sup>15</sup> or the separation of detrimental inclusions (MnS) from the steel melt <sup>16</sup>. There is an ongoing discussion in literature about the mechanisms being responsible for these beneficial effects. Recent experimental and numerical investigations demonstrated that electric currents can cause strong forced flows in the conducting melt due to the interaction between the electric current and the self-induced magnetic field <sup>5, 17</sup>. As known from electromagnetic stirring, the occurrence of forced flows can lead to the formation of macrosegregation. Precious little attention has been paid until now to the solute distribution in castings solidifying under the influence of electric current. This article is devoted to investigations of the distribution of eutectic phase in Al-7wt-%Si castings under the impact of forced flow induced by pulsed electric currents.

## **2. Experimental procedure**

### **2.1 Solidification experiment**

The Al-7wt-%Si hypoeutectic phase (nominal composition) was prepared by melting Al (99.99 wt-%) and Si (99.999 wt-%) in a clay-graphite crucible. After addition of 200 ppm of the modifier Sr the melt was cast into cylindrical samples having a diameter of 50 mm. After solidification individual pieces were cut to a height of 60 mm corresponding to a weight of 310 g. Subsequently, the preparatory sample was put into a double-walled stainless steel mould which is schematically shown in figure 1. The mould is closed by a stainless lid and the inner wall of the mould was coated by the electrically non-conducting boron nitride (BN) to avoid a closure of the electrical currents in the wall. A set of three NiCr-Ni thermocouples and a pair of parallel stainless steel cylindrical electrodes (diameter of 8 mm) were immersed into the solidifying melt and fixed at the lid. The thermocouples encased by Al<sub>2</sub>O<sub>3</sub> protecting tubes were vertically located along the axis of the mould for monitoring the temperature field during the solidification. The two parallel electrodes were arranged vertically at both sides of the mould axis in a distance of 36 mm and dipped into the melt up to a depth of 10 mm (see figure 1).

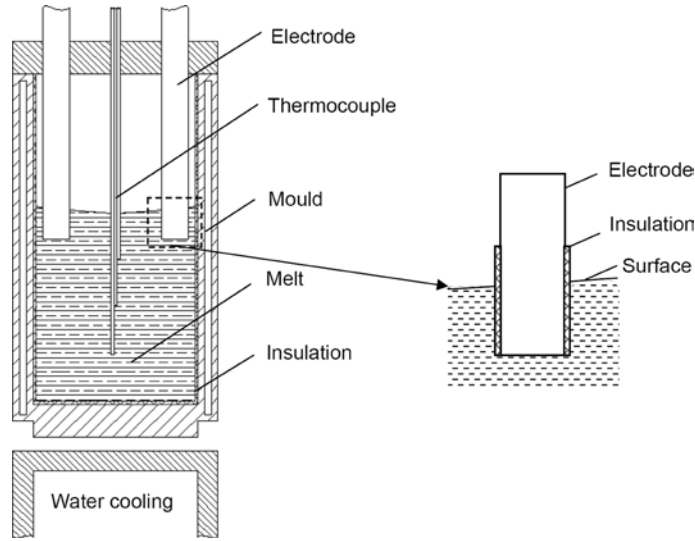


Figure 1: Schematic views of experimental solidification setup.

The alloy was remelted in a resistance furnace (Carbolite, Gpc 1300) and held at a temperature of 1023K for 45 mins. Then, the temperature was reduced to 993K applying a holding time of 30 mins. After the temperature treatment the mould was removed from the furnace and put on a water-cooled copper chill having a temperature of 293K for initiating the solidification process. The cooling of sample and the treatment by the electric current was triggered at the same time. The electric current was powered off when the sample was cooled to the eutectic point (about 846K). More details with respect to the experimental procedure can be found in <sup>17</sup>. The power supply pe86CWD (plating electronic) was used to inject the electric current. In the present study, a pulsed electric current (ECP) with rectangular form was applied. Respective electric current parameters are shown in table 1. The pulsed electric current is characterized by three parameters: the current amplitude  $I_p$ , the frequency  $f$  and the pulse length  $t_p$ . The resulting energy input supplied by ECP can be expressed by the effective value of the current amplitude  $I_{eff}$  <sup>17</sup>:

$$I_{eff} = I_p \sqrt{t_p \cdot f} \quad (1)$$

Table 1: Electric current parameters employed for solidification experiments

	Electric current pulse						
Intensity (A)	120	120	240	120	240	480	480
Frequency (Hz)	50	100	50	200	100	100	200
Pulse length (ms)	0.5	1	1	2	2	1	0.5
$I_{eff}$ (A)	19	38	54	76	107	152	152

## 2.2 Metallography

Solidified samples were cut along three sections as shown in figure 2. Section (S1) represents the midplane containing the electrode positions, whereas section (S2) corresponds to the perpendicular midplane. Additional examinations were done on section (S3) optionally. All sections were ground and polished from 6  $\mu\text{m}$  to 1  $\mu\text{m}$ , and then directly examined under an optical microscope (MeF4, Leica Microsystems, Wetzlar). From one cross section 482 single micrographs with the size of 2.88 mm $\times$ 2.16 mm were created.

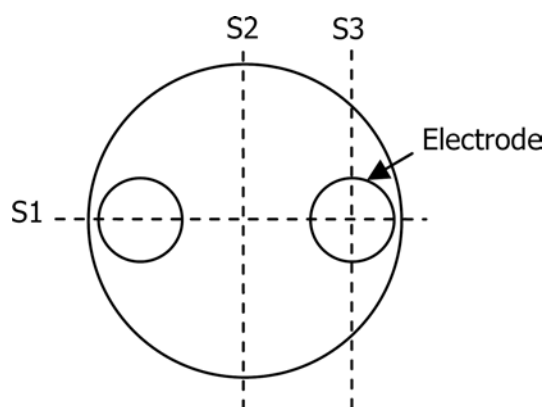


Figure 2: Schematic view of the sectioned planes.

As shown in figure 3a, the microstructure of the as-solidified Al-7wt-%Si hypoeutectic phase consists of the primary Al phase (light gray) and the eutectic phase (dark gray). Pores appear in the picture as black spots. The phase analysis was performed using the software package ANALYSIS FIVE (Olympus Europe, Hamburg). A threshold method was applied to separate both phases for determining the area percentage of the eutectic phase ( $C_e[\%]$ ) for each single picture. The area fraction covered by the pores was subtracted. Figure 3b contains a processed image showing both phases in different colors.

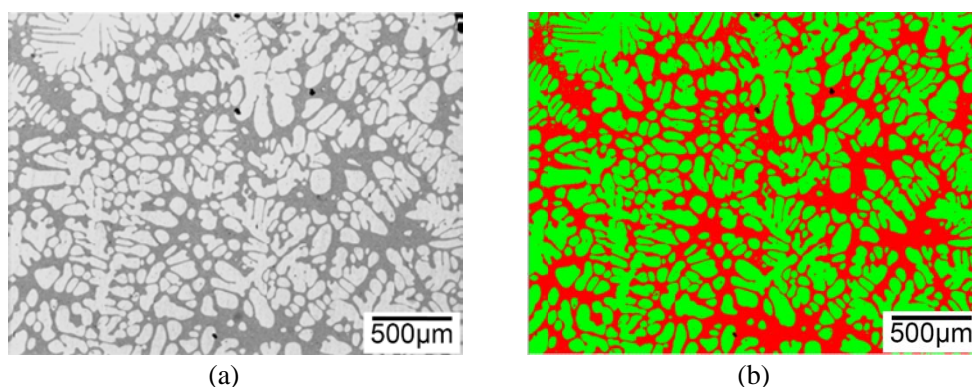


Figure 3: Typical microstructure of solidified Al - 7 wt % Si hypoeutectic phase: (a) grey-value image (light micrograph), (b) colored image.

### 3. Results

Figure 4 presents the distribution of eutectic phase in the section (S1) for the reference case of a sample solidified without ECP treatment. The eutectic phase appears to be distributed almost homogeneously among the entire section except for a small zone near the top of the sample between the electrodes (zone 1 in figure 4). The corresponding micrograph reveals that this depletion of the eutectic portion can be attributed to an insufficient feeding of the interdendritic zone by eutectic phase. Due to shrinkage the area between the dendrites of the primary phase is partly occupied by a large number of pores. Figure 4 also shows an exemplary micrograph representing the other regions on the section where the phases are homogeneously distributed. From this observation, we can conclude that the eutectic phase is distributed almost homogeneous in a sample which is solidified without applied electric current.

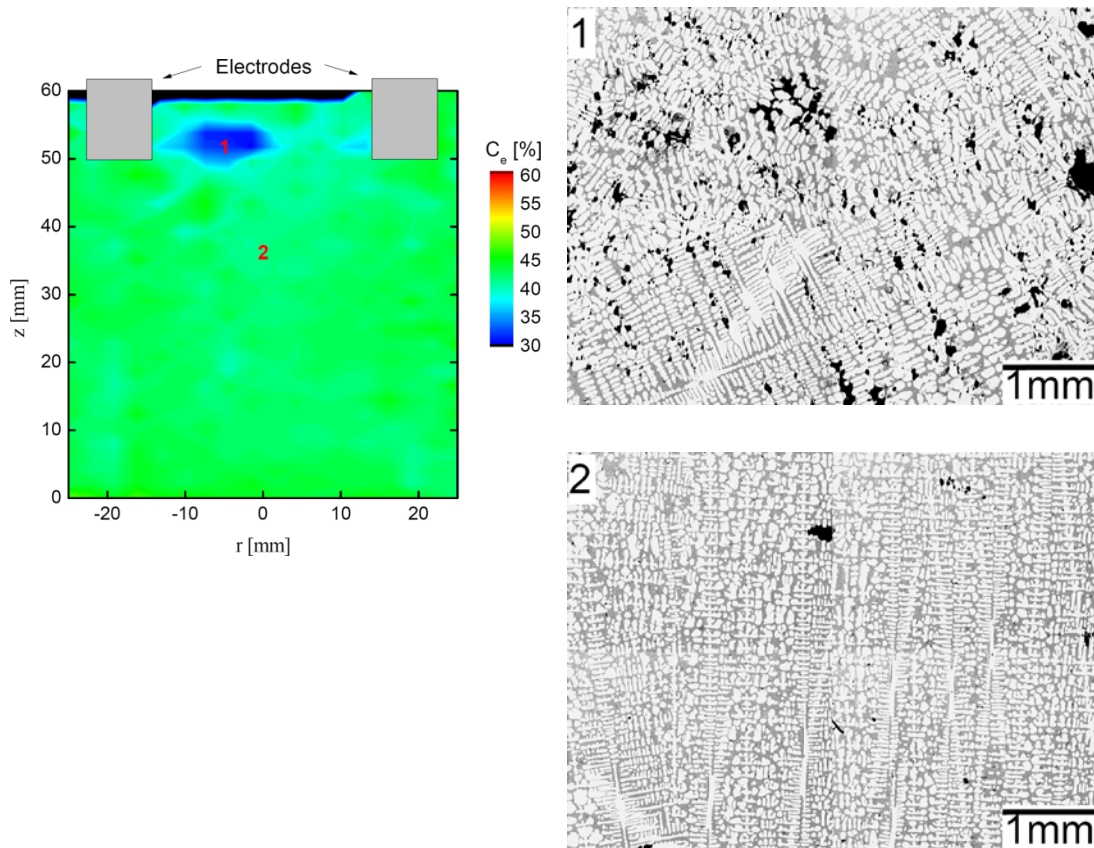


Figure 4: Measurements of the distribution of eutectic phase at section (S1) of a sample solidified without applying any electric current and respective micrographs taken at positions marked in the color plot.

The situation found in a sample treated by ECP at  $I_p = 480$  A,  $f = 200$  Hz,  $t_p = 0.5$  ms is shown in figure 5. Here, the analysis discloses the existence of various regions showing significantly higher or lower amounts of eutectic phase as the mean value over the cross section. Areas of positive macrosegregation are created at the top region of the sample between the positions of the electrode, while local regions of negative macrosegregation occur in regions beneath of the electrodes. The corresponding micrographs representing the various zones reveal the existence of larger inter-dendritic areas filled with eutectic phase along the top of the cell or a densification of the primary phase in isolated zones at lower positions. Moreover, it is worth to note that the number of pores is distinctly lower as in the non-treated case shown in figure 4. This could be explained by the melt stirring effect of ECP which was demonstrated by the reference<sup>17</sup>. Apparently, the stirring within the solidifying melt mitigates the problem of porosity due to insufficient feeding of the interdendritic zones by eutectic liquid.

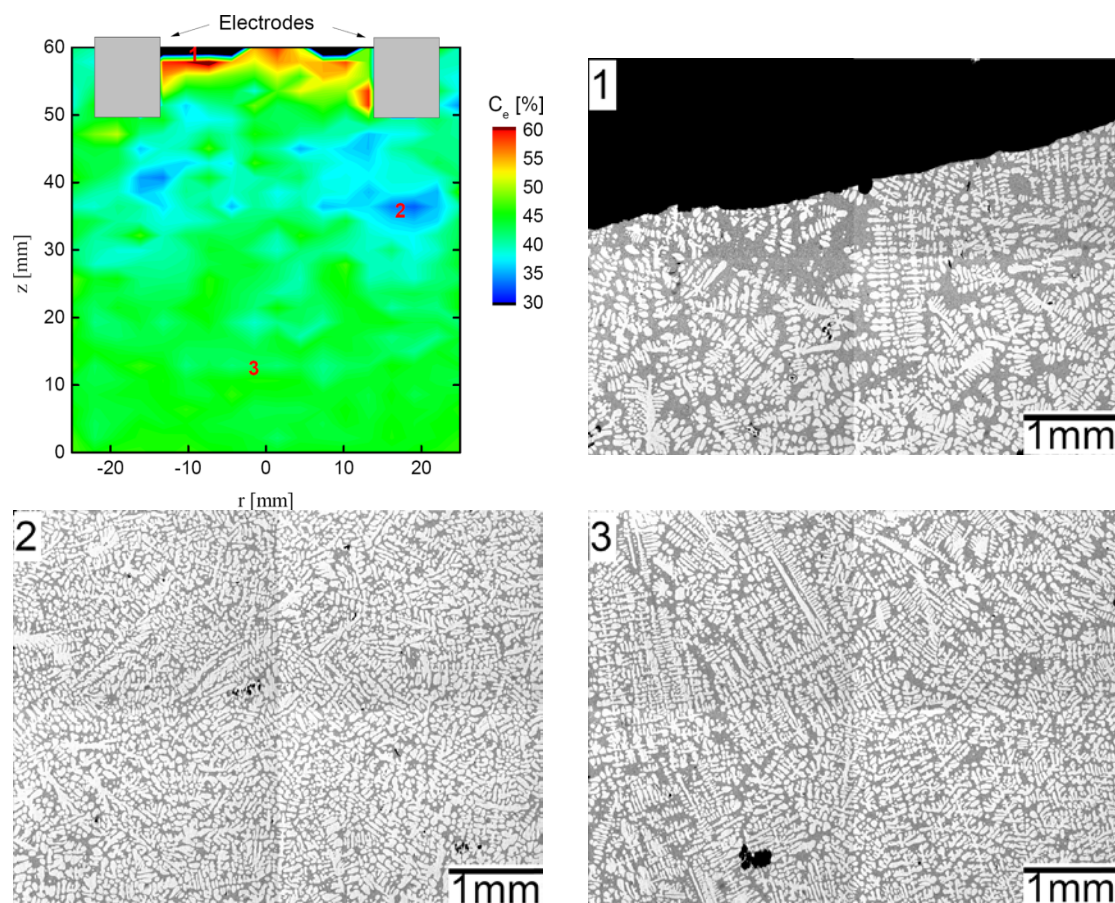


Figure 5: Measurements of the distribution of eutectic phase at section (S1) of a sample solidified under the influence of a pulsed electric current ( $I_p = 480$  A,  $f = 200$  Hz,  $t_p = 0.5$  ms,  $I_{eff} = 152$  A) and respective micrographs taken at positions marked in the color plot.

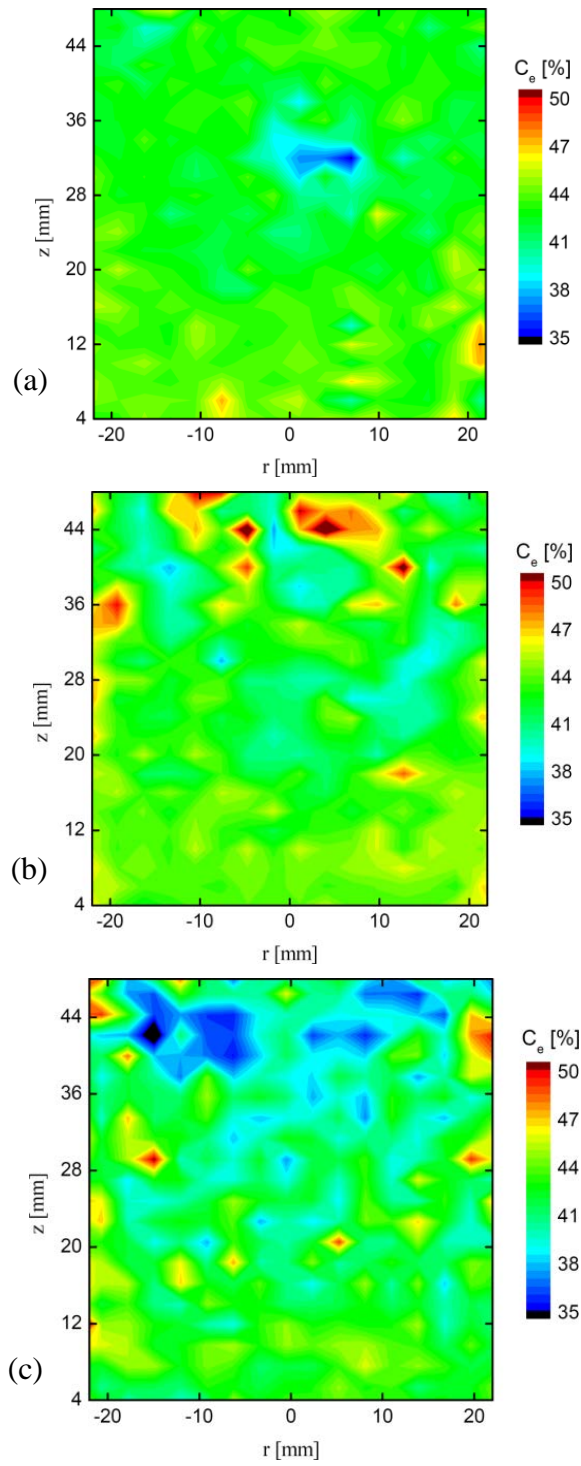


Figure 6: Measurements of the eutectic phase distribution at section (S2): (a)  $I_{eff} = 19$  A, (b)  $I_{eff} = 76$  A, (c)  $I_{eff} = 152$  A.



Analogue measurements of the phase distribution have been done in the perpendicular plane (S2). Figure 6 displays three samples which were treated by ECP at different values of the effective electric current. It becomes obvious, that the number of segregation freckles increases with increasing  $I_{eff}$ . However, characteristic pattern of segregation zones are not found, that means it is hard to determine specific regions where positive or negative segregation preferably emerges. In particular, a dominating positive segregation can be observed in figure 6(b) for the upper part of the sample. This trend is not further amplified by an increase of the electric current, instead the sign of segregation goes into reverse (see figure 6(c)).

In order to obtain a quantitative measure for describing the effect of  $I_{eff}$  on the development of the macrosegregation we define the variance ( $\sigma^2$ ) of the eutectic phase content on a particular section which is composed by a large number of single micrographs (see section 2). This value was calculated as follows:

$$\sigma^2 = \frac{1}{N} \sum_{i=1}^N (X_i - \bar{X})^2 \quad (2)$$

where  $X_i$  is the eutectic phase content in each single micrograph, and  $\bar{X}$  is the mean value representing  $N$  micrographs. The analysis in this study is focusing on the phase distribution in section (S2) using 432 single micrographs. The region at the top of sample was not taken into account because of the non-negligible concentration of pores due to shrinkage there. As already demonstrated in figure 4 the porosity will distort the validity of the results. Figure 7 shows the relationship between the variance ( $\sigma^2$ ) of eutectic phase content measured on section (S2) and the effective value of the electric current ( $I_{eff}$ ). One can observe a rising variance with growing value of  $I_{eff}$ , in other words the phases become more irregular distributed with increasing energy input.

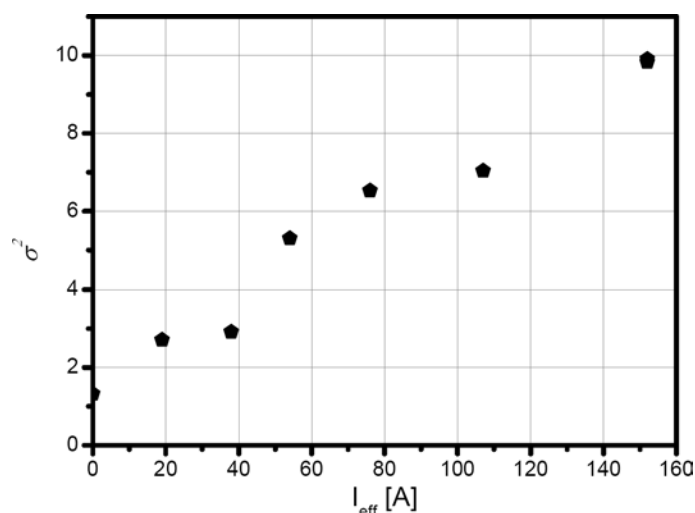


Figure 7: Influence of the effective electric current  $I_{eff}$  on the variance  $\sigma^2$  of the eutectic phase content measured at the section (S2).

#### 4. Discussion

It is widely accepted that the occurrence of macro segregation in as-solidified castings is caused by the relative motion between the solid phase and the liquid phase during the solidification process<sup>2, 3</sup>. A recent paper considered an identical experimental setup as used in this study and revealed a dominating role of forced convection with respect to grain refinement occurring in Al-Si alloys which are exposed to electric current pulses during solidification<sup>17</sup>. The interaction between the applied current and its own induced magnetic field causes a Lorentz force which produces an electro-vortex flow. An important factor is the existence of radially diverging electric currents directly at the tips of the electrodes. Their superposition with the induced azimuthal magnetic field generates maximum values of an axially aligned Lorentz force. This strong downwards Lorentz force just below the electrodes drives a flow in form of two descending jets. A recirculating flow occurs close to the cylinder walls within the lateral interspace on both sides of the electrodes<sup>18</sup>.

It has been found by previous investigations that dominating large-scale flow structures within the melt can cause characteristic segregation pattern. For instance, channel segregates develop because of thermo-solutal convection in the mushy zone<sup>19, 20</sup>. Roplekar & Dantzig<sup>21</sup> showed that the application of an RMF leads to macrosegregations in radial and axial direction. In particular, an enrichment of the eutectic phase was found on top and in the central region of cylindrical ingots. This finding is confirmed by other researchers<sup>8, 9, 22</sup>. This phenomenon can be attributed to the secondary flow inside the liquid phase. This secondary flow forms a vortex near the solidification front carrying solute which is rejected ahead of the mushy zone towards the middle of the sample. This advection of solute-rich liquid depleted is responsible for the development of a liquid channel on the axis of rotation inside of the mushy zone. Similarly, typical segregation freckles are reported for the application of a TMF. An enrichment of solute was observed near the axis or the side walls to depend on whether an upwards or downwards traveling field was applied<sup>7, 8</sup>.

Against this background it seems to be surprising that reproducible segregation patterns are not observed in the ECP experiments considered here, although the two downwards oriented jets below the electrodes form a large-scale, quasi-steady and dominating flow pattern. This contradiction could be resolved by the following explanation. In our case the jets impinge frontally on the mushy zone. This situation does not result in a horizontal, predominantly unidirectional flow along the solidification front which provides a continuous solute transport towards the center or the side walls. Moreover, the configuration of a strong melt flow aligned anti-parallel with respect to the growth direction of the solidification front seemingly promotes a transition from columnar-to-equiaxed growth (CET). Rather small values of  $I_{eff}$  proved to be sufficient for achieving an almost completely equiaxed grains structure<sup>17</sup>. The segregation in ingots that exhibit a fine-equiaxed grain structure is obviously different compared to columnar growth and is still an open field for research<sup>23</sup>

because the convection does not solely affect the solute transport, but, it will also determine the trajectories of the free-moving crystals.

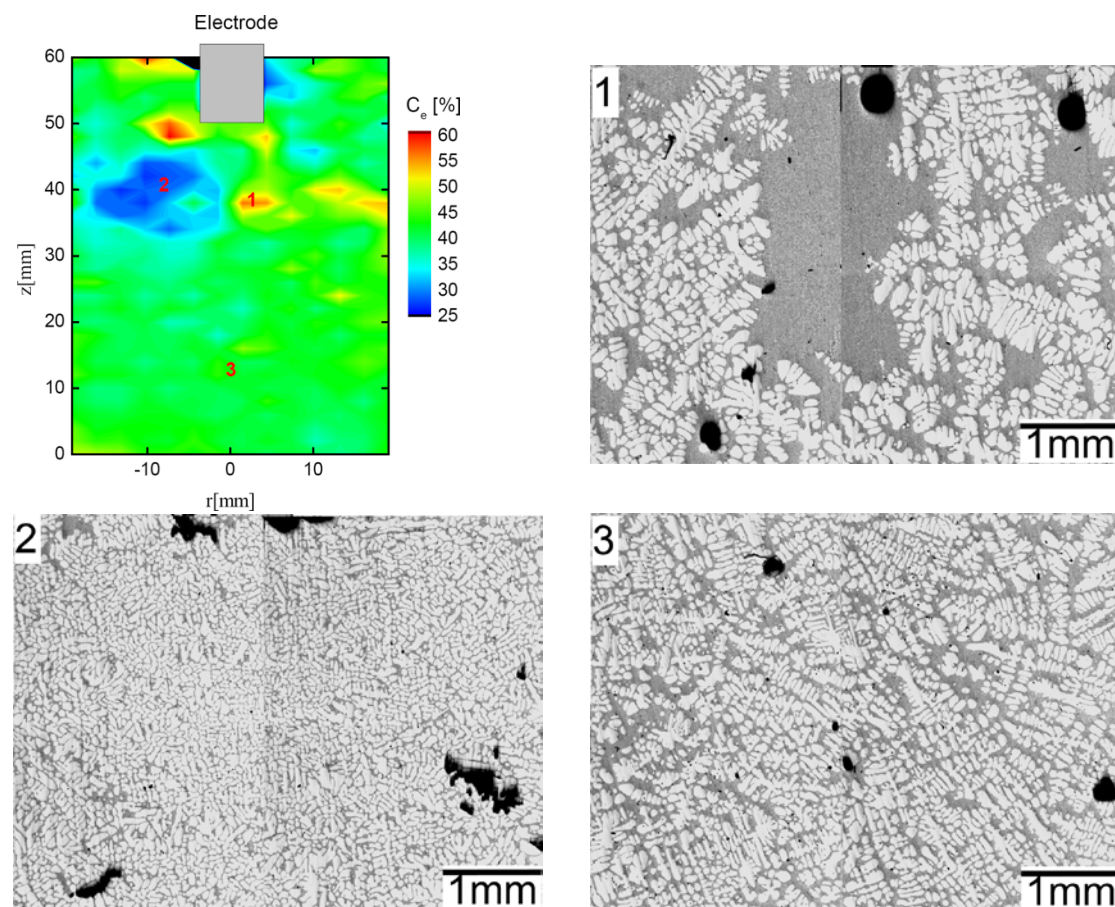


Figure 8: Measurements of the distribution of eutectic phase at section (S3) of a sample solidified under the influence of a pulsed electric current ( $I_p = 480$  A,  $f = 200$  Hz,  $t_p = 0.5$  ms,  $I_{eff} = 152$  A) and respective micrographs taken at positions marked in the color plot.

For further analysis we considered the microstructure on section (S3) in the area below one electrode where the jet flow is dominant. Figure 8 shows the phase distribution for a sample with ECP treatment ( $I_p = 480$  A,  $f = 200$  Hz,  $t_p = 0.5$  ms,  $I_{eff} = 152$  A). It becomes obvious that the bottom half of the sample remains almost unaffected by the ECP treatment whereas an alternating appearance of several zones of either positive or negative segregation can be observed in the upper part. As already seen in the other section (S1), the manifestation of positive segregation arises from individual spots solely filled by eutectic phase. Zones of negative segregation are characterized by a very dense structure of primary dendrites. The third micrograph shows an exemplary image taken from the almost homogeneous part of the sample.

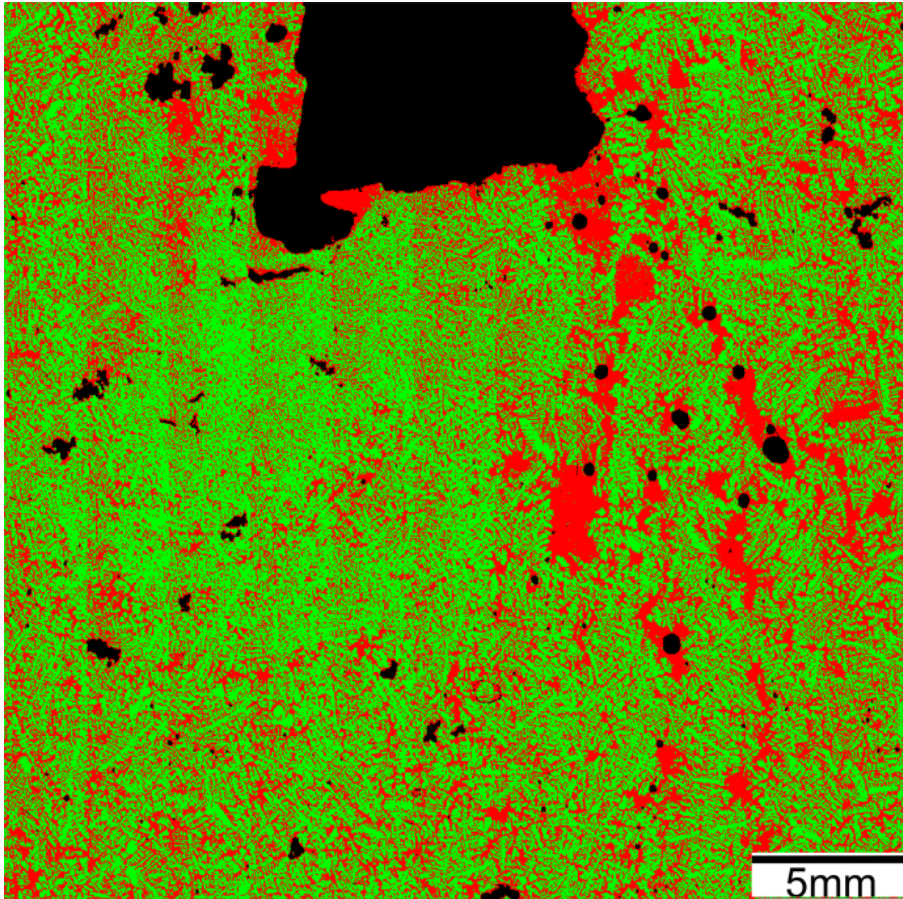


Figure 9: Solidified microstructure at section (S3), selected field of view of the sample shown in figure 8 (Area correspond to the area  $z = 26\text{mm}$  to  $54\text{mm}$  and  $r = -14.2\text{mm}$  to  $14.2\text{mm}$  in the color plot).

The colored image in figure 9 allows for a more detailed view on the solidified structure. It shows the upper part of section (S3) around the electrode position. The uneven distribution of eutectic phase beneath the electrode indicates a non-symmetric flow field in this area. It is reasonable to assume that the jet flow occurring under such conditions can be considered as turbulent and three-dimensional. Moreover, additional uncertainties could be caused by side effects like an uneven wetting of the front plane of the electrode by the liquid metal. The resulting distribution of the electrical currents is difficult to predict under such circumstances, however, a significant deflection and displacement of the jet is very likely. This phenomenon could be the reason that the segregation pattern found in various specimen differ significantly. Probably, the final appearance of the segregation pattern shown in figure 9 became manifest during the final state of the solidification process when the solidification came close to the electrode position. In this stage the deflected jet would create a vortex beneath the electrode which causes a washing out of solute in the left side of the image. The solute will be conveyed to the right hand site where it forms segregation freckles. Such a mechanism has already been observed in the reference <sup>4</sup>.

## 5. Conclusion

This paper presents an experimental study of macrosegregation in Al-7wt-%Si alloys solidified under the influence of electric current pulses (ECP). Under such conditions the solidification process is significantly affected by electromagnetically driven convection which is caused by the interaction of divergent electric currents at the electrodes and the induced magnetic field. In the case of two parallel electrodes immersed into the melt at the top of the sample the electromagnetic force generate a characteristic flow pattern which is composed of two downward jets below the electrodes and a weaker recirculating flow in the bulk. Obviously, the jet flow impinging frontally on the growing mushy zone promotes a disintegration of the columnar zone and a growth of free equiaxed crystals.

Although a distinct flow structure exists under the experimental conditions considered here we do not observe the formation of characteristic segregation pattern. Strong variations of the phase distributions are observed between the respective samples. A reproducible trend was found showing increasing variations of the composition within the samples with growing value of  $I_{eff}$  which represents a measure of the energy input by ECP. The irregular appearance of segregation zones in the samples can explained by the following reasons.

- The solidification proceeds mainly in the regime of equiaxed growth of free-moving crystals.
- The flow is turbulent and three-dimensional and does not show continuous flows perpendicular to a growing solidification front which is prone an accumulation of solute in certain areas of the samples.
- Further side effects like an uneven wetting of the electrodes by the liquid metal may contribute to a hardly foreseeable flow structure.

The formation of macrosegregation as considered here appears to be a rather complex phenomenon which requires further investigation for achieving a better understanding.

## Acknowledgement

The research is supported by the German Helmholtz Association in form of the Helmholtz-Alliance "LIMTECH". Yunhu Zhang is very grateful to the China Scholarship Council (CSC) for funding the scholarship under the grant 2011689010.

## References

1. M. E. Glicksman: 'Principles of solidification', 2011, Springer.
2. C. Beckermann: 'Modelling of macrosegregation: applications and future needs', *Int. Mater. Rev.*, 2002, **47**(5), 243-261.
3. M. C. Flemings and G. E. Nereo: 'Macrosegregation. PT. 1', *AIME Met. Soc. Trans.*, 1967, **239**(9), 1449-1461.
4. S. Boden, S. Eckert, and G. Gerbeth: 'Visualization of freckle formation induced by forced melt convection in solidifying GaIn alloys', *Mater. Lett.*, 2010, **64**(12), 1340-1343.
5. Y. Zhang, X. Miao, Z. Shen, Q. Han, C. Song, and Q. Zhai: 'Macro segregation formation mechanism of the primary silicon phase in directionally solidified Al-Si hypereutectic phases under the impact of electric currents', *Acta Mater.*, 2015, **97**, 357-366.
6. G. Zimmermann, A. Weiss, and Z. Mbaya: 'Effect of forced melt flow on microstructure evolution in AlSi7Mg0.6 alloy during directional solidification', *Mater. Sci. Eng. A*, 2005, **413**, 236-242.
7. K. Zaidat, T. Ouled-Khachroum, G. Vian, C. Garnier, N. Mangelinck-Noël, M. D. Dupouy, and R. Moreau: 'Directional solidification of refined Al-3.5 wt% Ni under natural convection and under a forced flow driven by a travelling magnetic field', *J. Cryst. Growth*, 2005, **275**(1), e1501-e1505.
8. A. Noepfel, A. Ciobanas, X. D. Wang, K. Zaidat, N. Mangelinck, O. Budenkova, A. Weiss, G. Zimmermann, and Y. Fautrelle: 'Influence of forced/natural convection on segregation during the directional solidification of Al-based binary alloys', *Metall. Mater. Trans. B*, 2010, **41**(1), 193-208.
9. B. Willers, S. Eckert, P. A. Nikrityuk, D. Rübiger, J. Dong, K. Eckert, and G. Gerbeth: 'Efficient melt stirring using pulse sequences of a rotating magnetic field: Part II. Application to solidification of Al-Si alloys', *Metall. Mater. Trans. B*, 2008, **39**(2), 304-316.
10. J. C. Jie, Q. C. Zou, J. L. Sun, Y. P. Lu, T. M. Wang, and T. J. Li: 'Separation mechanism of the primary Si phase from the hypereutectic Al-Si alloy using a rotating magnetic field during solidification', *Acta Mater.*, 2014, **72**, 57-66.
11. M. Gao, G. H. He, F. Yang, J. D. Guo, Z. X. Yuan, and B. L. Zhou: 'Effect of electric current pulse on tensile strength and elongation of casting ZA27 alloy', *Mater. Sci. Eng. A*, 2002, **337**(1), 110-114.
12. J. Li, J. H. Ma, Y. L. Gao, and Q. J. Zhai: 'Research on solidification structure refinement of pure aluminum by electric current pulse with parallel electrodes', *Mater. Sci. Eng. A*, 2008, **490**(1), 452-456.
13. X. L. Liao, Q. J. Zhai, J. Luo, W. J. Chen, and Y. Y. Gong: 'Refining mechanism of the electric current pulse on the solidification structure of pure aluminum', *Acta Mater.*, 2007, **55**(9), 3103-3109.
14. J. H. Ma, J. Li, Y. L. Gao, and Q. J. Zhai: 'Grain refinement of pure Al with different electric current pulse modes', *Mater. Lett.*, 2009, **63**(1), 142-144.
15. J. H. Ma, J. Li, Y. L. Gao, L. X. Jia, Z. Li, and Q. J. Zhai: 'Improving the carbon macrosegregation in high-carbon steel by an electric current pulse', *Met. Mater. Int.*, 2009, **15**(4), 603-608.
16. X. F. Zhang, W. J. Lu, and R. S. Qin: 'Removal of MnS inclusions in molten steel using

- electropulsing', *Scr. Mater.*, 2013, **69**(6), 453-456.
17. D. Rübiger, Y. H. Zhang, V. Galindo, S. Franke, B. Willers, and S. Eckert: 'The relevance of melt convection to grain refinement in Al-Si alloys solidified under the impact of electric currents', *Acta Mater.*, 2014, **79**, 327-338.
  18. S. Franke, D. Rübiger, V. Galindo, Y. Zhang, and S. Eckert: 'Investigations of electrically driven liquid metal flows using an ultrasound Doppler flow mapping system', *Flow Meas. Instrum.*, 2015.
  19. N. Streat and F. Weinberg: 'Macrosegregation during solidification resulting from density differences in the liquid', *Metall. Trans.*, 1974, **5**(12), 2539-2548.
  20. J. Sarazin and A. Hellawell: 'Channel formation in Pb-Sn, Pb-Sb, and Pb-Sn-Sb alloy ingots and comparison with the system NH<sub>4</sub>Cl-H<sub>2</sub>O', *Metall. Trans. A*, 1988, **19**(7), 1861-1871.
  21. J. A. D. J.K. Roplekar: 'A study of solidification with a rotating magnetic field', *Int. J. Cast Met. Res.*, 2001, **14**, 79-98.
  22. P. Nikrityuk, K. Eckert, and R. Grundmann: 'A numerical study of unidirectional solidification of a binary metal alloy under influence of a rotating magnetic field', *Int. J. Heat Mass Tran.*, 2006, **49**(7), 1501-1515.
  23. G. Lesoult, V. Albert, B. Appolaire, H. Combeau, D. Daloz, A. Joly, C. Stomp, G. Grün, and P. Jarry: 'Equi-axed growth and related segregations in cast metallic alloys', *Sci. Technol. Adv. Mater.*, 2001, **2**(1), 285-291.